Precision Timing with the CMS MIP Timing Detector

IOP Conf. Series: Journal of Physics: Conf. Series 1162 (2019) 012035 doi:10.1088/1742-6596/1162/1/012035

Precision Timing with the CMS MIP Timing Detector

Cristián H. Peña on behalf of the CMS Collaboration
Fermi National Accelerator Laboratory, Batavia, IL, US
California Institute of Technology, Pasadena, CA, US

E-mail: cmorgoth@fnal.gov

Abstract. The Compact Muon Solenoid (CMS) detector at the CERN Large Hadron Collider (LHC) is undergoing an extensive Phase II upgrade program to prepare for the challenging conditions of the High Luminosity LHC (HL-LHC). A new timing layer is designed to measure minimum ionizing particles (MIPs) with a time resolution of 30 ps and hermetic coverage up to a pseudo-rapidity of $|\eta|$=3. This MIP Timing Detector (MTD) will consist of a central barrel region based on LYSO:Ce crystals read out with SiPMs and two end-caps instrumented with radiation-tolerant Low Gain Avalanche Detectors (LGADs). The precision time information from the MTD will reduce the effects of the high levels of pile-up expected at the HL-LHC and will bring new and unique capabilities to the CMS detector. The time information assigned to each track will enable the use of 4D-vertexing which will render a 5-fold pile-up reduction thus recovering the current conditions. Precision timing will also enable new time-based isolations and improved b-tagging algorithms. All of this translates into a 20% gain in effective luminosity when looking at di-Higgs boson events decaying to a pair of b -quarks and two photons. We present the current status and ongoing R&D of the MTD, including implications on the physics reach at the HL-LHC and test beam results.

1. Introduction

The primary goal of the Phase-2 upgrade for the High-Luminosity LHC (HL-LHC) is to maintain the excellent performance of the CMS detector in efficiency, resolution, and background rejection for all final state particles and physical quantities used in data analyses. The CMS Upgrade Technical Proposal [1] presents, and the Scope Document [2] further specifies, a detailed upgrade plan to deploy an improved CMS detector by 2026, at the start of the HL-LHC operation [3]. It identifies changes necessary to withstand radiation damage effects and describes upgrades of the CMS components needed to overcome the challenge posed by the high rate of concurrent collisions per beam crossing (pileup) at the HL-LHC.

The LHC will operate at a stable luminosity of 5.0×10^{34} cm^{-2}s^{-1}, yielding 140 pileup collisions by continuously tuning the beam focus and the crossing profile during a fill. An ultimate scenario, with 7.5×10^{34} cm^{-2}s^{-1} luminosity and 200 pileup collisions per beam crossing, would provide 40% more accumulated data. At 140 or 200 pileup collisions, a hard interaction, one that probes energy scales of order 0.1–1 TeV, occurs in less than 1% of the total number of interactions simultaneously recorded by the detector. The spatial overlap of tracks and energy deposits from these collisions can degrade the identification and the reconstruction of the hard interaction, and can increase the rate of false triggers.

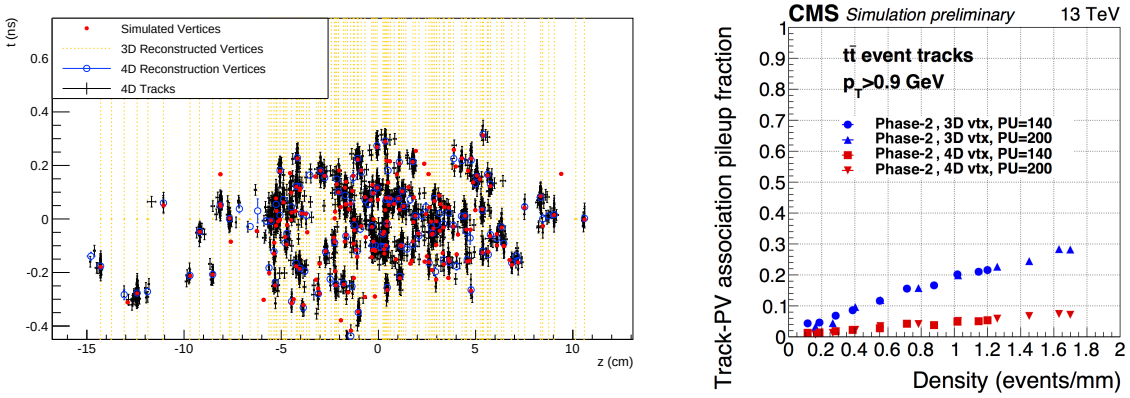

Figure 1: Left: simulated and reconstructed vertices in a 200 pileup event assuming a MIP timing detector covering the barrel and endcaps. The vertical lines indicate 3D-reconstructed vertices, with instances of vertex merging visible throughout the event display. Right: rate of tracks from pileup vertices incorrectly associated with the primary vertex of the hard interaction normalized to the total number of tracks in the vertex.

Pileup mitigation in CMS relies upon particle-flow event reconstruction [4], which removes from relevant quantities charged tracks inconsistent with the vertex of interest, and neutral deposits in the calorimeters with ansatz-based statistical inference techniques like PUPPI [5]. The high spatial granularity of the subdetectors will enable the upgraded CMS detector to separate vertices, to identify the hard collision, and to measure signal particles with good efficiency in the offline analyses [1, 2]. However, in the transition from 140 to 200 pileup events, the probabilities of spatial overlap grow in all subdetectors, and subsequently particle-flow algorithms begin to fail at a substantial rate. The resulting degradation in resolutions, efficiencies, and misidentification rates at 200 pileup events impacts several physics measurements [2, 6].

The timing upgrade of the CMS detector will improve the particle-flow performance at high pileup to a level comparable to the Phase-1 CMS detector, exploiting the additional information provided by the precision timing of both tracks and energy deposits in the calorimeters. In the time domain, pileup collisions at the HL-LHC will occur with an RMS spread of approximately 180–200 ps, constant during the fill and uncorrelated with the line spread along the beam line. Slicing the beam spot in consecutive 30 ps exposures effectively reduces the number of vertices down to current LHC conditions, thereby recovering the Phase-1 quality of event reconstruction. In addition to the enhanced timing capabilities of the calorimeters [1], this approach requires a dedicated detector for precision timing of minimum ionizing particles (MIPs): the MIP timing detector (MTD) [7].

The event display in Fig. 1 (left panel) visually demonstrates the power of space-time reconstruction in 200 pileup collisions, using a time-aware extension (4D) of the deterministic annealing technique adopted in vertex reconstruction by the CMS experiment [8]. According to simulation, instances of vertex merging are reduced from 15% in space to 1% in space-time. Another quantitative measure of the performance improvement is shown in the right panel of Fig. 1, showing the rate of tracks from pileup vertices incorrectly associated with the hard interaction vertex as a function of the line density of vertices. The addition of track-time information with 30 ps precision reduces the wrong associations to a level comparable to that of the current LHC (vertex density of to about 0.3 mm^{-1}). The performance of b-jet identification, which relies on vertex reconstruction, is enhanced. The removal of pileup tracks

Table 1: Representative signals for Higgs boson measurements and SUSY searches used to map each specific detector requirement into the relative performance gain at the analysis level (analysis impact) and in the measured physical quantity (physics impact).

Signal	Detector requirement	Analysis impact	Physics impact
$H \to \gamma\gamma$	30 ps photon and track timing • barrel: central signal • endcap: improved time-zero and acceptance	$S/\sqrt{B}$: $+20\%$ - isolation efficiency $+30\%$ - diphoton vertex	$+25\%$ (statistical) precision on cross section
VBF+ $\mathbf{H}\to\tau\tau$	30 ps track timing • barrel: central signature • endcap: forward jet tagging • hermetic coverage: optimal $E_{\mathrm{T}}^{\mathrm{miss}}$ reconstruction	$S/\sqrt{B}$: $+30\%$ - isolation efficiency $+30\%$ - VBF tagging $+10\%$ - mass ($E_{\mathrm{T}}^{\mathrm{miss}}$) resolution	$+20\%$ (statistical) precision on cross section (upper limit or significance)
HH	30 ps track timing • hermetic coverage	signal acceptance : $+20\%$ b-jets and isolation efficiency	Consolidate **HH** searches
$\chi^{\pm}\chi^{0} \to$ W$^{\pm}$H+$E_{\mathrm{T}}^{\mathrm{miss}}$	30 ps track timing • hermetic coverage: $E_{\mathrm{T}}^{\mathrm{miss}}$	$S/\sqrt{B}$: $+40\%$ - reduction of $E_{\mathrm{T}}^{\mathrm{miss}}$ tails	$+150$ GeV mass reach
Long-lived particles	30 ps track timing • barrel: central signature	mass reconstruction of the decay particle	unique sensitivity to split-SUSY and SUSY with compressed spectra

from the isolation cones improves the identification efficiency for isolated leptons and photons, which are key signatures of many processes of interest for the HL-LHC program. Similarly, the reconstruction of spatially extended objects and global event quantities that are vulnerable to pileup, such as jets and $E_{\mathrm{T}}^{\mathrm{miss}}$, is also significantly improved. All of this consistently motivates a precision timing detector in the barrel and in the endcaps, with about 30 ps resolution in order to enhance the HL-LHC physics reach.

2. Impact of precision timing on the HL-LHC physics program

The CMS physics program at the HL-LHC will target a very wide range of measurements, including in-depth studies of the Higgs boson properties and direct searches for physics beyond the standard model (BSM). The added value of a timing detector, quantified in terms of improved vertex identification, acceptance extension for isolated objects, improved $E_{\mathrm{T}}^{\mathrm{miss}}$ resolution, and pileup jet rate reduction, makes a significant impact on the CMS physics program across several channels. A synopsis is presented in Table 1, where detector requirements are mapped into analysis and physics impacts.

The characterization of the Higgs boson properties, with precision measurements of the Higgs boson couplings to standard model (SM) particles, and the search for rare SM and BSM decays, will benefit from the improved acceptance for isolated objects, and in the case of $H \to \gamma\gamma$ decays from improved vertex identification. Another crucial measurement at the HL-LHC is di-Higgs production, and consequently the direct measurement of the Higgs self-coupling. In this case, precision timing increases the signal yields for constant background in $\mathbf{HH} \to \mathbf{b\bar{b}}\gamma\gamma$ by 17% from the barrel alone, and 22% with hermetic coverage (Fig. 2). Similar enhancements are predicted for other important Higgs boson signatures, ranging from 15–20% for $\mathbf{HH} \to 4$b to 20–26% for $\mathbf{H} \to \mathbf{ZZ} \to 4\ell$, for constant background. These acceptance extensions will provide improved precision in the measurement of rare decay modes and of statistically limited differential distributions, with sensitivity to Higgs boson pseudo-observables [9]. Figure 2 (middle panel) shows the relative improvement on signal efficiency for $\mathbf{H} \to \mathbf{ZZ} \to 4\ell$ with respect to the no-timing scenario and as a function of the Higgs rapidity. Efficiency improvements of 20-30% are observed in both barrel and endcap regions.

The sensitivity to several searches for new phenomena is largely driven by the $E_{\mathrm{T}}^{\mathrm{miss}}$

resolution, which determines the background level for several BSM signatures. The gain in the $E_{\mathrm{T}}^{\mathrm{miss}}$ resolution with track timing leads to a reduction of $\sim$ 40% in the tail of the $E_{\mathrm{T}}^{\mathrm{miss}}$ distribution above 130 GeV, which approximately offsets the performance degradation for SUSY searches in the transition from 140 to 200 pileup [2]. Additional benefits of the precision timing are anticipated in searches with multi-lepton final states due to the increased efficiency of the lepton isolation selection, and in signatures where a direct measurement of the time of flight (TOF) of heavy particles is exploited. For example, a TOF measurement in a detector in front of the calorimeters will reduce the model dependence in searches for Heavy Charged Stable Particles, now limited to particles that have little interactions with the calorimeters [10, 11]. Moreover, the track-time reconstruction opens a new avenue in searches for neutral long lived particles (LLPs), postulated in many extensions of the standard model like Split-SUSY, GMSB, RPV SUSY, Stealth SUSY, SUSY models with compressed mass spectra and many others discussed in [12] and references therein. The space-time information associated to the displaced decay vertex, will enable the kinematic reconstruction: for example, the direct measurement of the LLP mass (Fig. 2), thus boosting the sensitivity of such searches and providing a novel method to characterize any future discovery.

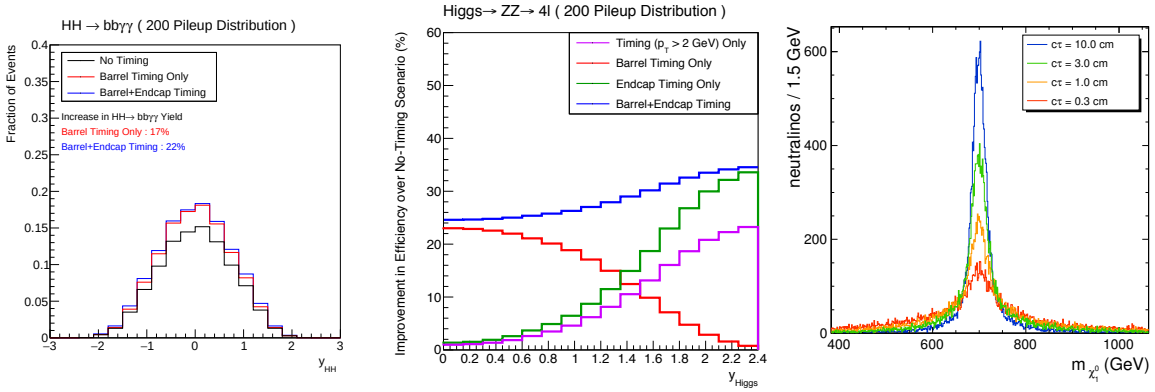

Figure 2: Left: impact on signal efficiency for $\mathbf{HH} \to \mathbf{b\bar{b}}\gamma\gamma$ for no-timing and timing scenarios. Middle: relative improvement on signal efficiency for $\mathbf{H} \to \mathbf{ZZ} \to 4\ell$ with respect to no-timing scenario. Right: mass peak of a 700 GeV neutralino reconstructed from the kinematic closure of the secondary vertex using time information with 30 ps resolution.

3. MIP Timing Detector

Figure 3 shows a simplified implementation in GEANT of the proposed layout integrated in the CMS detector. The MTD will comprise a barrel and an endcap region, with different technologies based on different performance, radiation, mechanics and schedule requirements and constraints:

- Cost effective design over a large area: Performance studies motivate the need of a hermetic coverage, with time resolution of order 30–40 ps for charged tracks throughout the detector lifetime.
- Integration constraints: A single layer device between the Tracker and calorimeters, covering up to $|\eta| \sim 3$, is imposed by space and integration constraints.
- Granularity: A channel area of order 1 cm^2 in the barrel, and varying in the endcaps down to 3 mm^2 at $|\eta| \sim 3$, yields a good compromise between low time response spread within a channel, low occupancy and low channel count. The channel occupancy is limited to a few

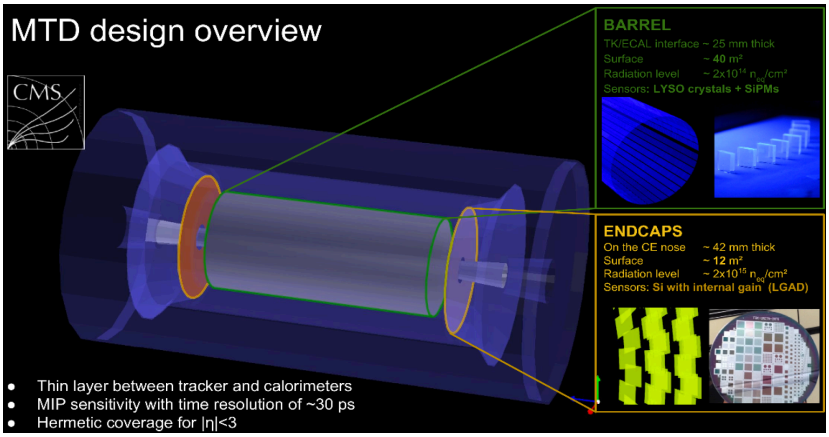

Figure 3: A simplified GEANT geometry of the timing layer implemented in CMSSW for simulation studies comprises a LYSO barrel (grey cylinder), at the interface between the Tracker and the ECAL, and two silicon endcap (orange discs) timing layers in front of the CE calorimeter.

percent, ensuring both a small probability of double hits, needed for unambiguous time assignment, and a manageable data volume.

- Radiation tolerance: The MTD must be able to operate efficiently up to an integrated luminosity of 4000 fb^{-1}, without any maintenance intervention for the barrel detector, whereas the endcap detector may be accessible during the HL-LHC era. Table 2 shows the expected particle fluence and radiation doses at possible timing layer locations, between the Tracker and the ECAL calorimeter, and in front of the neutron moderator of the endcap calorimeter.
- Marginal impact on the Tracker performance and design: The proposed design of the barrel timing layer requires the outer radius of the tracker to be reduced by up to 15 mm. This reduction in radius will make a negligible impact on the tracking performance (Section 3.1.1), but requires attention in terms of schedule and design (Section 4.1.1). Care must also be taken to prevent mechanical and thermal instabilities that may affect the Tracker alignment.
- Marginal impact on the calorimeter performance: In the current CMS detector, the electron and photon energy resolution is degraded by the amount of material in front of the calorimeters. The upgraded CMS Tracker is designed with significantly less material in the fiducial volume. The additional timing layer should be maintained thin enough not to deteriorate the performance of the calorimeters.
- Compliance with the CMS upgrade schedule: The Tracker and calorimeters upgrades constrain the MTD schedule. In particular, the available region in the barrel, at the interface between the Tracker and the calorimeter, has to be fully instrumented early in the Tracker integration phase, currently scheduled for 2022, to enable the assembly of the Tracker on schedule for the start of the Phase-2 (2025). This constraint narrows down the choice to a mature, essentially ready, technology for the barrel timing layer.

Five technologies were investigated and studied in dedicated beam tests and radiation exposures, building upon and extending long-standing R&D programs [14, 15, 16, 17, 18, 19, 20, 21, 22, 23, 24]. Crystal scintillators read out with silicon photomultipliers (SiPMs) [14, 15, 16] and silicon sensors with internal gain [17, 18, 19] emerged, respectively, as a mature technology for the barrel and a viable technology for the endcap timing layers.

Table 2: Radiation doses and fluences at the timing layers after 4000 fb^{-1} from the online BRIL radiation tool [13]. The fluence is normalized to 1 MeV neutron equivalent in silicon.

Region	η	R (cm)	z (cm)	Fluence (cm^{-2})	Dose (kGy)
barrel	0.0	117	0	1.7×10^{14}	16
barrel	1.15	117	170	1.9×10^{14}	21
barrel	1.45	117	240	2.0×10^{14}	25
endcap	1.6	127	304	1.1×10^{14}	25
endcap	2.0	84	304	2.4×10^{14}	75
endcap	2.5	50	304	6.6×10^{14}	260
endcap	3.0	30	304	1.7×10^{15}	690

3.1. Barrel Timing Layer

For the barrel timing layer (BTL), we propose to adapt the present Tracker Support Tube (TST) design by instrumenting the current location of the thermal screen with a thin, actively cooled, standalone detector, based on lutetium-yttrium orthosilicate crystals activated with cerium (LYSO:Ce) read out with SiPMs. Both LYSO based scintillators and SiPMs devices are mature technologies, with production and assembly procedures well established and standardized in industry. The R&D for a precision timing application is well advanced, and small prototypes consisting of LYSO:Ce crystals read out with SiPMs have been proven capable of achieving time resolution below 30 ps (see Fig. 4) [25]. Both the crystals and the SiPM are proven to be radiation tolerant up to a neutron equivalent fluence of 2×10^{14} cm^{-2}, when cooled to below -30 °C. The read-out electronics can be adapted from existing positron emission tomography applications with time-of-flight (TOF-PET) measurement [26, 27, 28], which is read out upon an external (Level-1) trigger. The barrel timing layer will cover the pseudorapidity region up to $|\eta| = 1.48$ with a total active surface of about 40 m^2. The fundamental detecting cell will consist of a thin LYSO:Ce crystal with about $\sim 12 \times 12$ mm^2 cross-section coupled to a 4×4 mm^2 SiPM. The crystal thickness will vary between about 3.7 mm ($|\eta| < 0.7$) and 2.4 mm ($|\eta| > 1.1$), to level the slant depth crossed by particles from the interaction point. The proposed layout has no impact on the upgraded designs and schedules of the Tracker and the ECAL.Additionally, a preliminary simulation study using a with a 4 mm thick LYSO:Ce layer, i.e. thicker than in the reference design, also indicates no significant impact on the performance of shower reconstruction and energy resolution in the ECAL.

3.2. Endcap Timing Layer

The endcap region can be instrumented with a hermetic, single layer of MIP-sensitive silicon devices with high time resolution, with a pseudorapidity acceptance from about $|\eta| = 1.6$ to $|\eta| = 2.9$. The choice for the placement of this detector within the CMS experiment is driven by the necessity to ensure its accessibility throughout the HL-LHC operation. Therefore, we propose to place the endcap timing layer (ETL) in its own independent, thermally isolated volume on the nose of the endcap electromagnetic calorimeter, at a distance of about 3 m from the interaction point. Sensor modules will be mounted on two sides of two double-sided disks in order to provide hermetic coverage. The active sensor area is a little over 6 m^2 per endcap.

We propose to use planar silicon devices with internal gain, since the technology selected for the barrel cannot be extended to the endcap, due to radiation tolerance limitations. The silicon sensors have intrinsic gain, in order to overcome capacitance and other noise sources and thus achieve 30–50 ps timing resolution for minimum ionizing particles (see Fig. 4). As a reference design we propose to build the fast-timing detector based on Low-Gain-Avalanche-Diodes (LGAD) [18, 19], which are also considered for a fast-timing layer in the very forward region ($2.4 < |\eta| < 4.8$) of the ATLAS experiment [29]. The radiation tolerance studies, though still in progress, indicate promising performance of about 30 and 50 ps at fluences corresponding

to $|\eta| \simeq 2.5$ and 3.0, respectively, at the end of the HL-LHC operation. Achieving good time performance at low-gain requires cell sizes typically less than 3 mm^2, to limit the sensor capacitance. While the barrel timing layer should be installed before the Tracker, the time schedule to assemble the endcap discs can extend toward the end of the LHC long shutdown LS3 (2025), thus providing additional time to complete the R&D plan.

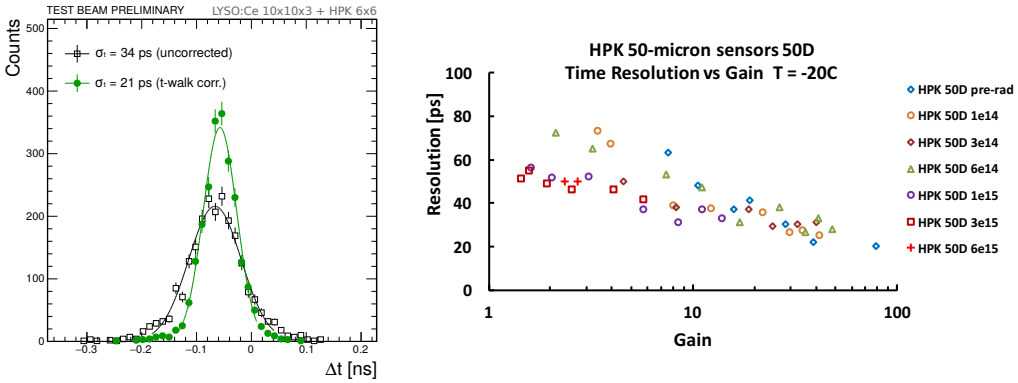

Figure 4: Left: distribution of the time difference in a pair of LYSO:Ce tiles exposed to a 3 mm wide beam of MIPs hitting the centre of the tiles. Results before and after time walk correction for $10 \times 10 \times 3$ mm^3 crystals read out with 6×6 mm^2 HPK SiPMs are shown. Right: time resolution for HPK LGAD sensors as a function of internal gain, different radiation levels are shown with different markers.

4. Summary and Future Considerations

The addition of a precise timing detector, able to efficiently tag charged particles, will significantly suppresses the effect of pileup on all object-level observables at the HL-LHC. This suppression yields significant and democratic improvements to many physics analyses – including Higgs, BSM, LLPs, and di-Higgs physics – by increasing signal efficiencies or reducing the width of residual distributions for discriminating variables.

The MIP timing detector is a conceptual realization for such precision timing detector at the HL-LHC. The MTD is composed of two subsystems based in different sensor technologies: SiPMs+LYSO:Ce for the barrel region and LGADs for the endcap region. The technology choices were driven by performance, radiation, mechanics and schedule requirements and constraints. Both sensor technologies are mature and proven to achieve ∼30–50 ps time resolutions.

While full readout of the MTD is not possible, because of bandwidth constraints, it may be possible for the MTD to play a crucial role in the Level-1 trigger. The MTD Level-1 trigger information can be formed in the off-detector electronics from the data of regions of interest (ROI). The read out of the ROIs can be seeded by a Level-0 request from the Tracker, muon or the calorimeter triggers. The impact of timing on the CMS triggers, technical implications for the MTD read-out electronics and for the Level-1 trigger latency, as well as a complete description of the mechanical specifications and detector performance will be described forthcoming in the Technical Design Report (TDR) from CMS.

References

[1] "Technical Proposal for the Phase-II Upgrade of the CMS Detector," Tech. Rep. CERN-LHCC-2015-010. LHCC-P-008, CERN, Geneva, Jun 2015.

[2] "CMS Phase II Upgrade Scope Document," Tech. Rep. CERN-LHCC-2015-019. LHCC-G-165, CERN, Geneva, Sep 2015.
[3] G. Apollinari, O. Brning, T. Nakamoto, and L. Rossi, "High Luminosity Large Hadron Collider HL-LHC," *CERN Yellow Report*, p. 1, 2015.
[4] "Particle-flow reconstruction and global event description with the cms detector," *JINST*, vol. 12, p. P10003, 2017.
[5] D. Bertolini, P. Harris, M. Low, and N. Tran, "Pileup Per Particle Identification," *JHEP*, vol. 1410, p. 59, 2014.
[6] CMS Collaboration, "Updates on Performance of Physics Objects with the Upgraded CMS detector for High Luminosity LHC," CMS Performance Note CMS-DP-2016-065, 2016.
[7] CMS Collaboration, "Technical Proposal for a MIP Timing Detector in the CMS Experiment Phase 2 Upgrade," Tech. Rep. CERN-LHCC-2017-027. LHCC-P-009, 2017.
[8] S. Chatrchyan *et al.*, "Description and performance of track and primary-vertex reconstruction with the CMS tracker," *JINST*, vol. 9, p. P10009, 2014.
[9] D. de Florian *et al.*, "Handbook of LHC Higgs Cross Sections: 4. Deciphering the Nature of the Higgs Sector," 2016.
[10] CMS Collaboration, "Enhanced scope of a Phase 2 CMS detector for the study of exotic physics signatures at the HL-LHC," CMS Physics Analysis Summary CMS-PAS-EXO-14-007, 2016.
[11] O. Cerri, S. Xie, C. Pena, and M. Spiropulu, "Identification of Long-lived Charged Particles using Time-Of-Flight Systems at the Upgraded LHC detectors," 2018.
[12] A. Coccaro, D. Curtin, H. J. Lubatti, H. Russell, and J. Shelton, "Data-driven model-independent searches for long-lived particles at the LHC," *Phys. Rev. D*, vol. 94, p. 113003, 2016.
[13] CMS Collaboration, "FLUKA particle flux maps for CMS Detector," CMS Performance Note CMS-DP-2013-028, 2013.
[14] S. Gundacker, E. Auffray, B. Frisch, P. Jarron, A. Knapitsch, T. Meyer, M. Pizzichemi, and P. Lecoq, "Time of flight positron emission tomography towards 100 ps resolution with L(Y)SO: an experimental and theoretical analysis," *JINST*, vol. 8, p. P07014, 2013.
[15] D. Anderson, A. Apresyan, A. Bornheim, J. Duarte, C. Pena, A. Ronzhin, M. Spiropulu, J. Trevor, and S. Xie, "On timing properties of lyso-based calorimeters," *Nucl. Instrum. Meth. A*, vol. 794, p. 7, 2015.
[16] D. Anderson *et al.*, "Precision Timing Measurements for High Energy Photons," *Nucl.Instrum.Meth. A*, vol. 787, p. 94, 2015.
[17] S. N. White, "R&D for a Dedicated Fast Timing Layer in the CMS Endcap Upgrade," *Acta Phys. Pol. B Proc. Suppl.*, vol. 7, p. 743, 2014.
[18] G. Pellegrini *et al.*, "Technology developments and first measurements of Low Gain Avalanche Detectors (LGAD) for high energy physics applications," *Nucl. Instrum. Meth. A*, vol. 765, p. 12, 2014.
[19] N. Cartiglia *et al.*, "Design optimization of ultra-fast silicon detectors," *Nucl. Instrum. Meth. A*, vol. 796, p. 141, 2015.
[20] A. Ronzhin, S. Los, E. Ramberg, M. Spiropulu, A. Apresyan, S. Xie, H. Kim, and A. Zatserklyaniy, "Development of a new fast shower maximum detector based on microchannel plates photomultipliers (mcp-pmt) as an active element," *Nucl. Instrum. Meth. A*, vol. 759, p. 65, 2014.
[21] A. Ronzhin, S. Los, E. Ramberg, A. Apresyan, S. Xie, M. Spiropulu, and H. Kim, "Direct Tests of Micro Channel Plates as the Active Element of a New Shower Maximum Detector," *Nucl. Instrum. Meth. A*, vol. 795, p. 52, 2015.
[22] L. Brianza *et al.*, "Response of microchannel plates to single particles and to electromagnetic showers," *Nucl. Instrum. Meth. A*, vol. 797, p. 216, 2015.
[23] A. Barnyakov, M. Barnyakov, L. Brianza, F. Cavallari, V. Ciriolo, D. Del Re, S. Gelli, A. Ghezzi, C. Gotti, P. Govoni, *et al.*, "Beam test results on the detection of single particles and electromagnetic showers with microchannel plates," *Nucl. Instrum. Meth. A*, vol. 845, p. 471, 2017.
[24] T. Papaevangelou *et al.*, "Fast Timing for High-Rate Environments with Micromegas," in *4th International Conference on Micro Pattern Gaseous Detectors - MPGD2015 Trieste, Italy, October 12-15, 2015*, 2016.
[25] A. Benaglia, S. Gundacker, P. Lecoq, M. T. Lucchini, A. Para, K. Pauwels, and E. Auffray, "Detection of high energy muons with sub-20 ps timing resolution using L(Y)SO crystals and SiPM readout," *Nucl. Instrum. Meth. A*, vol. 830, p. 30, 2016.
[26] M. D. Rolo *et al.*, "TOFPET ASIC for PET applications," *JINST*, vol. 8, p. C02050, 2013.
[27] M. D. Rolo *et al.*, "A low-noise CMOS front-end for TOF-PET," *JINST*, vol. 6, p. P09003, 2011.
[28] A. D. Francesco *et al.*, "TOFPET2: a high-performance ASIC for time and amplitude measurements of SiPM signals in time-of-flight applications," *JINST*, vol. 11, p. C03042, 2016.
[29] "ATLAS Phase-II Upgrade Scoping Document," Tech. Rep. CERN-LHCC-2015-020. LHCC-G-166, CERN, Geneva, Sep 2015.